Original Article

Avicenna Journal of Medical Biotechnology
Volume 18, Issue 2, 147-156
https://doi.org/10.18502/ajmb.v18i2.21507

Bioactive Silver Nanoparticles Coated with Curcumin Inhibit Angiogenesis through MMP-9 and Cox-2 Down-Regulation

Tayebe Ramezani Farzin [1*] and Mohammad Nabiuni [2]

1. Farzanegan Campus of Semnan University, Semnan, Iran
2. Department of Biology, Kharazmi University, Tehran, Iran

Abstract

Background: Inhibition of angiogenesis is an attractive approach in cancer therapy. Both curcumin and silver nanoparticles (AgNPs) have demonstrated anti-angiogenic properties; however, the the poor water solubility of Curcumin and the side effects of AgNPs adversely affect their activity.

Methods: In this study, AgNPs coated with curcumin (Cur-AgNPs), was used to improve aqueous-phase solubility of curcumin and decrease the side effects of AgNPs. Afterwards, treatment with curcumin enhanced the anti-angiogenic activity of Cur-AgNPs. The nanoparticles were synthesized as both reducing and stabilizing agents. Evaluation of anti-angiogenesis was assessed *in vitro* using Human Umbilical Vein Endothelial Cells (HUVECs) and *in vivo* through the Chorioallantoic Membrane (CAM) assay. Data were analyzed by one-way ANOVA with Tukey's multiple comparison test.

Results: Synthesized Cur-AgNPs have an average diameter of 39 *nm*, with spherical shapes and an absorbance peak at 450 *nm* in the UV-visible spectrum. Cur-AgNPs showed a negative zeta potential. EDAX and FTIR confirmed the conjugation of curcumin with AgNPs. *In vitro* anti-angiogenesis assays demonstrated that Cur-AgNPs reduced the viability of HUVECs, an Inhibitory Concentration (IC50) value of 13 *µg/ml*. DAPI and acridine orange/propidium iodide staining revealed a significant increase in apoptotic cells following treatment with Cur-AgNPs. The expression of *Matrix Metalloproteinase 9* (*MMP-9*) and *Cyclooxygenase-2* (*COX-2*) was also inhibited in treated cells. *In vivo* anti-angiogenesis assays using the CAM model showed significant decrease in the number, length and hemoglobin content of CAM blood vessels.

Conclusion: Curcumin conjugated with AgNPs may represent a promising strategy to enhance the therapeutic potential of both AgNPs and curcumin. However, further investigations, particularly regarding safety and biocompatibility of Cur-AgNPs, is needed in this field.

*** Corresponding author:**
Tayebe Ramezani Farzin, Ph.D.,
Farzanegan Campus of Semnan University, Semnan, Iran
Tel: +98 2333464884
E-mail:
tayeberamezani@semnan.ac.ir
Received: 25 Oct 2025
Accepted: 2 Feb 2026

Keywords: Angiogenesis, Curcumin, Nanoparticles, Silver
To cite this article: Ramezani Farzin T, Nabiuni M. Bioactive Silver Nanoparticles Coated with Curcumin Inhibit Angiogenesis through MMP-9 and Cox-2 Down-Regulation. Avicenna J Med Biotech 2026;18(2):147-156.

Introduction

Angiogenesis is a significant concept in cancer-related research, since the formation of new blood vessels is critical to the survival and metastasis of tumor cells. Anti-angiogenic therapy is one of the most critical strategies in combating cancer, as it inhibits or disrupts the growth of tumor blood vessels that provide essential nutrients and oxygen to maintain cancer cell activity [1]. Due to the high mutation rate of tumor cells, they become resistant to anti-cancer drugs, while the low mutation rate of normal endothelial cells leads to their low resistance to such medications [2]. Anti-angiogenesis agents are used in the treatment of some diseases that involve abnormal blood vessel growth under noncancerous conditions, such as macular degeneration [3]. The FDA has approved certain drugs that have anti-angiogenic activity, including pazopanib, sorafenib, and sunitinib. Furthermore, the combination of angiogenesis inhibitors with additional therapies, especially chemotherapy, has reportedly increased their effectiveness [4].

Curcumin is an active ingredient of *Curcuma longa* with numerous pharmacological activities, such as anti-carcinogenic, anti-inflammatory, antioxidant, and anti-angiogenic properties. Curcumin functions as an angiogenic inhibitor by effectively suppressing several pro-angiogenic proteins, including Vascular Endothelial Growth Factor (VEGF) and basic Fibroblast Growth Factor (bFGF). It was also reported that curcumin reduces the viability of Human Umbilical Vein Endothelial Cells (HUVECs) [5,6]. However, poor bioavailability of curcumin significantly limits its therapeutic activity, due to low absorption, rapid metabolism and fast elimination from the system [7,8]. Researchers have attempted to both improve the solubility and targeted delivery of curcumin to cells. For instance, Zhang *et al* [9] developed a photoresponsive self-microemulsifying system carrying curcumin to improve both solubility of curcumin and its delivery to the colon [9]. Ullah [10] formulated a photoactivated self-microemulsifying drug delivery system loaded with curcumin to provide a carrier for such hydrophobic molecules [10].

Recently, improving the bioavailability of curcumin using nanotechnology has become a significant concern among researchers. In the current work, an effort was made to increase the bioavailability of curcumin by designing a biological system. The medical properties of silver have been known for over 2,000 years [11]. In recent years, anti-angiogenic and anti-cancerous effects of AgNPs have also been considered [12,13]. This study aimed to develop curcumin coated silver nanoparticles (AgNPs) to decrease the side effects of AgNPs, enhancing nanoparticles stability and improving curcumin's solubility, and bioavailability.

Materials and Methods

Reagents

Curcumin (Sigma-Aldrich, United Kingdom), MTT [3-(4, 5-dimethylthiazol-2-yl)-2,5-diphenyltetrazolium bromide] (Sigma-Aldrich, United Kingdom), Acridine Orange (AO), and Ethidium Bromide (EB) (Sigma-Aldrich, United Kingdom), DAPI (4'-6-diamidino-2-phenylindole) (Sigma-Aldrich, United Kingdom), Annexin V/PI (Abcam, Germany), Caspase 9 assay kit (Abcam company, Germany), High Pure RNA Isolation Kit (Roche, Germany), cDNA Synthesis Kit (Fermentas, Germany), RPMI-1640 and and Fetal bovine serum (Invitrogen, United States). DMSO (dimethyl sulfoxide) (Merck, Germany), paraformaldehyde (Merck, Germany) and PCR kit (Parstous, Iran). HUVECs (Pastor cell bank, Iran), primers (Bioneers, Korea). All experiments were performed in at least three independent biological replicates.

Synthesis

The synthesis method of the Cur-AgNPs has been previously discribe by Ramezani *et al* in 2019 [14]. In the earlier work, their anti-cancer effects were evaluated, whereas in the present study, their anti-angiogenic properties were investigated. Briefly, Cur-AgNPs were synthesized by reducing an aqueous solution of $AgNO_3$ using curcumin as both the reducing and stabilizing agent. To this end, 500 *ml* of $AgNO_3$ (1 *mM*) was prepared, and 1 *ml* of curcumin (100 *mM*) was added to the solution and mixed thoroughly. The mixture was kept at room temperature until the color changed from yellow (curcumin) to brown, indicating the formation of Cur-AgNPs.

Characterization methods

The UV-visible absorbance spectra of Cur-AgNPs were recorded in the range of 300-700 *nm* using a spectrophotometer (Epoch Biotech, Winooski, VT, United States). The hydrodynamic size distribution and zeta potential of Cur-AgNPs were determined by Dynamic Light Scattering (DLS) at 25°*C*, using a medium viscosity of 0.89 *cP*, a fixed scattering angle of 90°, and a 678 *nm*, 90 *mW* laser (Cordovan, Vaso Particle, France). The morphology of the Cur-AgNPs was observed using Transmission Electron Microscopy (TEM, Hitachi, Tokyo, Japan). Energy- dispersive X-ray was performed to characterize the elemental composition (EDX, XL 30; Philips, Eindhoven, Netherlands).

In Vitro Anti-angiogenic Effects of Cur-AgNPs using Human umbilical vein endothelial cells

Cell culture: Human Umbilical Vein Endothelial Cells (HUVECs) were maintained in RPMI 1640 medium enriched with 10% FBS and 1% penicillin-streptomycin (100 *U/ml*). Cells were incubated at 37°*C* in a humidified environment containing 5% CO_2.

Cytotoxicity assay

MTT Cytotoxicity assay

MTT Solution Preparation: A stock solution of MTT was prepared by dissolving 10 *mg* of MTT powder in 2 *ml* of Phosphate-Buffered Saline (PBS, pH=7.4). The solution was sterilized by passing through a 0.22 *µm* syringe filter and stored at 4°*C* in the dark. Prior to use, the MTT stock solution was equilibrated to room temperature.

HUVECs were cultured in T-25 flasks using complete culture medium until approximately 80% confluence was reached. The cells were then detached using trypsin-EDTA, centrifuged, and resuspended in fresh medium. Cell density was determined using a hemocytometer and trypan blue exclusion. The required cell number was calculated, and an appropriate volume was taken from the stock suspension. Cells were seeded in 96-well plates at a density of 1×10^4 cells per well in 100 *µl* of complete medium.

Each treatment condition was performed in triplicate. The plates were incubated overnight at 37°*C* with 5% CO_2 to allow cell attachment and recovery to logarithmic growth phase. After 24 *hr*, the medium was replaced with fresh complete medium containing Cur-AgNPs at final concentrations of 5, 10, 15, 20, and 40 *µg/ml*. The cells were incubated for another 24 *hr* under the same conditions. Following treatment, the medium was carefully removed, and 50 *µl* of fresh medi-

um along with 5 *µl* of MTT solution (5 *mg/ml* in PBS) were added to each well. The plates were incubated at 37°*C* for 4 *hr* to allow the formation of insoluble formazan crystals. The supernatant was then discarded, and the formazan crystals were dissolved in 100 *µl* of DMSO per well. Absorbance was measured at 570 *nm* using a microplate reader (Epoch, Biotek, Winooski, VT, USA). Cell viability was expressed as a percentage of the untreated control using the formula:

Cell viability (%) = (A_treated/A_control) × 100.

Staining assays

AO/EB staining: HUVECs were cultured in 24-well plates at a density of 5×10^4 cells/well. After 24 *hr*, the cells were treated with 13 *µg/ml* of Cur-AgNPs (corresponding to the IC_{50}) for 24 *hr*. Subsequently, the cells were harvested, centrifuged, and resuspended in an equal volume of AO-EB solution. The samples were then examined under a fluorescence microscope (Olympus, Tokyo, Japan). AO/EB staining quantification using ImageJ.

Treated and control cells were collected. The cells were then stained with a mixture of acridine orange and ethidium bromide according to procedure described above. The number of total and viable cells was counted using ImageJ software. The percentage of viable cells was calculated as follows:

$$\%\ \text{of viable cells} = \frac{\text{Number of viable cells nuclei}}{\text{Total nuclei}} \times 100$$

At least three random microscopic fields per sample were analyzed, and the mean±Standard Deviation (SD) was reported. Statistical analysis was performed to compare the treatment groups with the control group.

DAPI staining: Endothelial cells were cultured in 24-well plates at a density of 5×10^4 cells/well and treated with 13 *µg/ml* of Cur-AgNPs (corresponding to the IC_{50}) for 24 *hr*. The treated cells were then fixed with 4% paraformaldehyde, stained with DAPI solution (1 *µg/ml*) for 60 *s*, and observed under a fluorescence microscope (Olympus, Tokyo, Japan) using a 488 *nm* filter.

DAPI staining quantification using ImageJ

The total number of nuclei in microscopic images of the samples was counted. Apoptotic nuclei were identified based on their morphological features, including condensed and fragmented shapes. The percentage of viable cells was calculated using the following formula:

$$\%\ \text{of viable cells} = \frac{\text{Number ofcells nuclei}}{\text{Total nuclei}} \times 100$$

Gene expression assay by semi-quantified PCR: The IMPACT of Cur-AgNPs on the expression of Matrix Metalloproteinase 9 (*MMP-9*) and Cyclooxygenase-2 (*COX-2*) genes in HUVECs, was determined using the quantification Reverse Transcription Polymerase Chain Reaction (RT-PCR). The effect of Cur-AgNPs on the expression levels of *MMP-9* and *COX-2* genes in HUVECs was evaluated using quantitative Reverse Transcription Polymerase Chain Reaction (qRT-PCR). Endothelial cells were cultured at a density of 5×10^6 cells 75 cm^2 flasks and treated with 13 *µg/ml* Cur-AgNPs for 24 *hr*. Total RNA was isolated and reverse-transcribed into complementary DNA (cDNA), which served as the template for PCR amplification with specific primers (Table 1). PCR reactions were carried out using a commercial kit (Parstuos, Iran) under the following conditions: initial denaturation at 94°*C* for 5 *min*, followed by 35 cycles of denaturation (94°*C*, 30 *s*), annealing (56°*C*, 30 *s*), and extension (68°*C*, 45 *s*), with a final elongation step at 72°*C* for 5 *min*. Amplified products were separated on 1.5% agarose gels and visualized using a gel documentation system (Unitec, Cambridge, UK). Band intensities were quantified using ImageJ software, and relative gene expression in treated cells was compared with that in untreated controls.

In-vivo assessment of ANT-angiogenic effects of Cur-AgNPs

Chick embryo chorioallantoic membrane assay: Fifty fertilized Ross chicken eggs were employed for the Chorioallantoic Membrane (CAM) assay and incubated at 37°C with 55-65% relative humidity throughout the experiment.

On the second day, a small window was created on each eggshell to access the CAM. On day 8 of incubation, in experimental groups, were treated with 10 *µl* of Cur-AgNPs at concentrations of 25, 50, 75, and 100 *µg/ml*. The treated eggs were then returned to the incubator. On day 12 of incubation, all eggs were examined and imaged using a stereomicroscope (Zeiss, Munich, Germany) equipped with a digital camera (Canon PowerShot G2).

Assessment of CAM vascularization and hemoglobin content

The vascularization network (number and length of blood vessels) surrounding the gelatin sponge was analyzed in all samples using ImageJ software. Additionally, the extent of vascularization was quantified based on the hemoglobin level in the CAM using the Drabkin method. Briefly, CAM tissues were homogenized for

Table 1. Primer sequence

Gene	Forward primer	Reverse primers
GAPDH	5' GGCCAAGAT CAT CCA TGA CAA CT3'	5'ACCAGGACATGAGCTTGACAA GT3'
COX-2	5'AAGCCTTGCCTCAGAGAGA	5'CTCGAGTGTGGGCTA
MMP-9	5' CTG CAT CCT CAG CAG GTTG 3'	5' GTC TCG GAT AGT CTT TAT CC 3'

15 *min*, and the homogenates were centrifuged at 5000 rpm for 5 *min*. The supernatant was mixed with 1 *ml* of Drabkin reagent. The absorbance of each sample was recorded at 546 *nm* using a spectrophotometer (Epoch Biotech, Winooski, VT, USA) according to the manufacturer's instructions.

Ethical approval

This study was approved by the Ethics Committee of the Faculty of Veterinary Medicine, Semnan University, with the ethical code IR.SU.REC.1404.22.

Statistical analysis

All experiments were conducted in at least in triplicate, and data are presented as mean±Standard Deviation (SD). Statistical analyses were performed using one-way analysis of variance (ANOVA) followed by Tukey's multiple comparison test. Differences were considered statistically significant at $p<0.05$.

Results

Synthesis and characterization OF Cur-AgNPs

As previously reported, Cur-AgNPs were successfully fabricated using curcumin as a reducing and capping agent. UV-visible spectroscopy revealed a distinct absorbance peak at 440 *nm*, confirming the formation of AgNPs. Transmission Electron Microscopy (TEM) showed that Cur-AgNPs were mostly spherical in shape with a uniform distribution, while DLS analysis demonstrated an average nanoparticle size of 39 *nm*. The AgNPs exhibited a zeta potential in the negative range of -10 to -30 *mV*, indicating good colloidal stability. This negative surface charge generates repulsive forces between individual Cur-AgNPs, preventing agglomeration and contributing to their stability in solution. These findings indicate that the synthesis process produces well-formed and stable AgNPs suitable for various applications, depending on their size and morphology (Figures 1A and 1C).

The similarity between the FTIR spectral patterns of free curcumin and the Cur-AgNPs verified successful conjugation of curcumin on the surface of Cur-AgNPs due to presence of curcumin's characteristic absorption bands in the FTIR spectra of the nanoparticles. This conjugation likely enhances the stability and physicochemical properties of the synthesized nanoparticles (Figure 1D). In addition, energy-dispersive X-ray spectroscopy was used to determine the elemental composition of Cur-AgNPs. The EDX spectra (Figure 1C) displayed prominent silver peaks, while the presence of oxygen and carbon peaks indicated successful conjugation of curcumin with the nanoparticles. These findings confirm the successful synthesis and interaction between curcumin and AgNPs (Figure 1E).

Anti-angiogenic effects and apoptosis induction of Cur-AgNPs on HUVECs

Cytotoxicity assay: The cytotoxic effects of Cur-AgNPs on HUVECs were evaluated using the MTT assay. The results demonstrated a clear dose-dependent decrease in cell viability, with an IC_{50} value of 13 *µg/ml* after 24 *hr* of treatment. Concentrations below 5 *µg/ml* did not significantly affect cell viability ($p\geq0.05$) indicating that low concentrations of Cur-AgNPs is nontoxic for the cells while, concentrations above 40 *µg/ml* induced rapid and pronounced cytotoxicity, leading cell death within the first hour after treatment ($p\leq0.001$; Figure 2). These finding suggest that Cur-AgNPs reduce endothelial cell viability and proliferation which in may suppress new blood vessel formation. These results support the anti-angiogenesis properties of Cur-AgNPs.

Morphological change observation

DAPI staining: DAPI is a fluorescent dye with high affinity that binds to AT-based pairs in DNA. DAPI staining was used to evaluate nuclear morphology change in HUVECs following treatment with 13 *µg/ml* Cur-AgNPs for 24 *hr*. Compared to untreated groups, Cur-AgNPs-treated cells exhibited characteristic hallmarks of apoptosis, including chromatin condensation, cell shrinkage, and apoptotic body formation (Figures 3A and 3C). Quantitative analysis of DAPI-stained cells showed that 30% of cells ($p=0.009$) in the nanoparticle-treated groups exhibited signs of apoptosis. In contrast, cells in the untreated control group remained healthy, with cell viability around 95%. The apoptosis index measured by DAPI staining may appear lower than the decrease in viability observed in the MTT assay, as MTT reflects metabolic activity while DAPI detects nuclear changes associated with apoptosis. Furthermore, cells that detach during apoptosis or late necrosis are usually lost during the washing and staining process, and therefore are not counted under the microscope. These findings confirm that Cur-AgNPs induce apoptosis in endothelial cells, potentially contributing to their anti- angiogenesis activity.

AO/EB staining: AO/EB staining was used to assess the effects of 13 *µg/ml* Cur-AgNPs on HUVECs. In this assay cells exhibited green fluorescence, whereas apoptotic cells displayed bright orange to red nuclei due to chromatin condensation and DNA fragmentation. After 24 *hr* of exposure to 13 *µg/ml* of Cur-AgNPs, the number of apoptotic (orange) cells increased in Cur-AgNPs treated cells compared to the untreated control.

Quantitative analysis of AO/EB -stained cells showed that the percentage of viable cells in the treated group decreased by approximately 37%, and the presence of yellow and orange hues in the stained images indicated induction of apoptosis. In contrast, cells in the untreated control group mostly displayed green fluorescence, with cell viability remaining at about 98%. The Viale cells in treated groups reduced significs ($p=0007$). Representative fluorescence images clearly revealed apoptotic morphological features, including nuclear condensation and membrane blebbing in the treated cells. In this type of staining, as in DAPI staining, the percentage of dead cells may appear lower

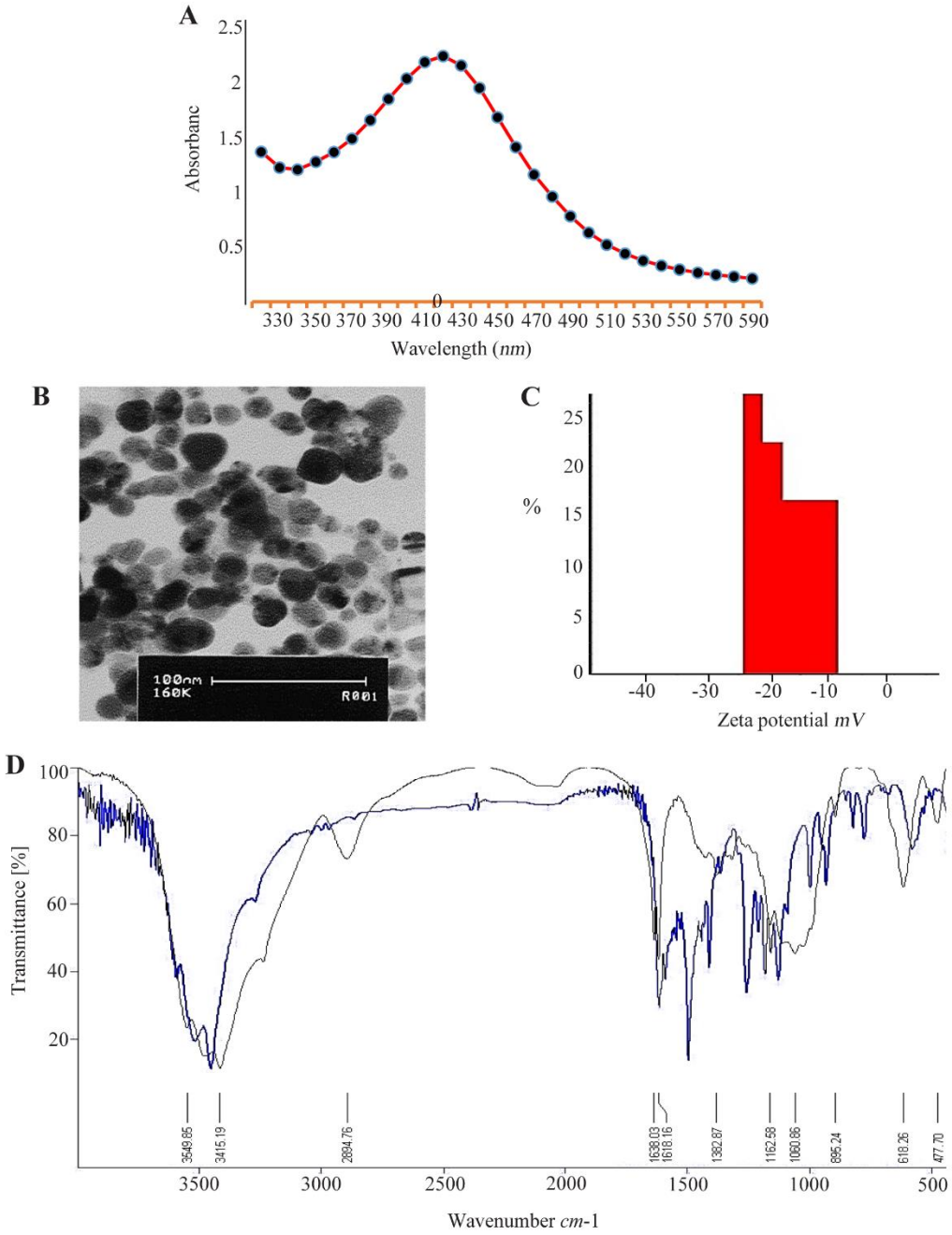

Figure 1. Synthesis and characterization of Cur-AgNPs.
A) UV–visible absorption spectrum of Cur-AgNPs. The absorption peak observed around 450 *nm* confirms the formation of silver nanoparticles.
B) TEM image of Cur-AgNPs showing spherical nanoparticles with good dispersion.
C) Zeta potential curve of Cur-AgNPs. The nanoparticles exhibited a negative potential ranging from -10 to -30 *mV*, which prevents their aggregation.
D) Comparison of FTIR spectra of curcumin (blue) and Cur-AgNPs (black). The similarity between the two spectra indicates that curcumin is bound to the silver nanoparticles.

than that measured by the MTT assay. This is because cells in the late stages of cell death are often lost during the staining and washing procedures. Nevertheless, the relative increase in cell death in treated groups compared to the control is clearly observable. This result corroborates the DAPI staining data, supporting anti-angiogenic activity of Cur-AgNPs (Figure 2D and 2F).

Gene expression analysis: Semi-quantitative RT-PCR was employed to examine the expression of *COX-2* and *MMP-9* in HUVECs treated with 13 *µg/ml* of Cur-AgNPs. The results, indicated a significant downregulation *MMP-9* expression in HUVECs (to 69% relative expression) compared to untreated control groups (p= 0.005). Similarly, *COX-2* expression decreased mark-

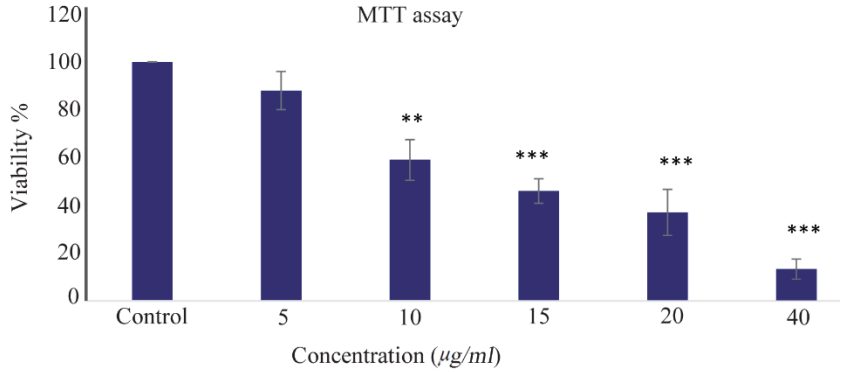

Figure 2. Viability assay by MTT assay. Cytotoxic effects of Cur-AgNPs on HUVECs after 24 *hr*. The results demonstrated that cell viability decreased in a dose-dependent manner in HUVECs treated with Cur-AgNPs compared with the control group. The data are presented as mean±SD (***p≤0.001).

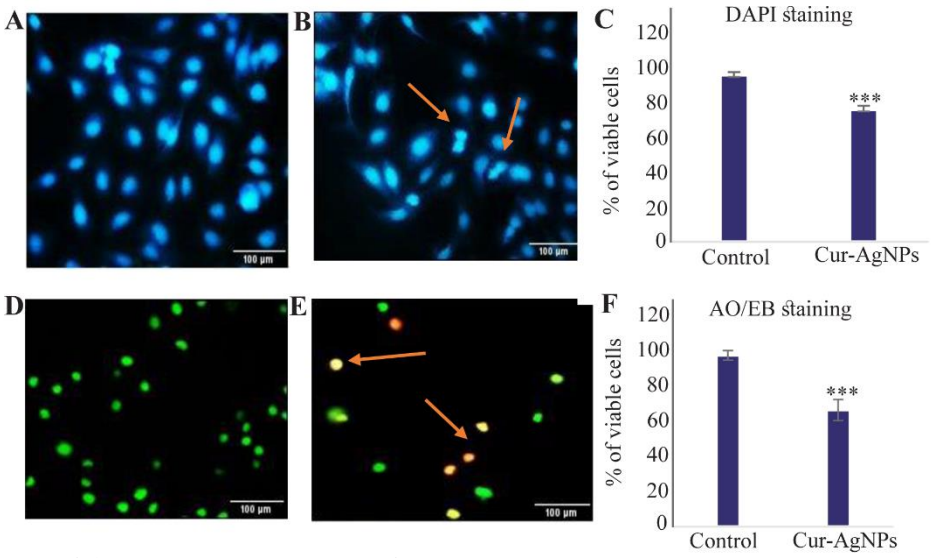

Figure 3. Cur-AgNPs (13 *μg/ml*) induced apoptosis in HUVECs after 24 *hr*.
A) Non-treated control group stained with DAPI. In this group, the cell nuclei remained intact, and no evidence of cell death was observed.
B) Cur-AgNP-treated group stained with DAPI. Evidence of apoptosis, such as nuclear condensation and disruption of cellular integrity, was observed.
C) Quantification of live cells in the treated sample compared with the untreated control. The graph shows an increased proportion of dead cells in the treated group compared with the control.
D) Control group stained with Acridine Orange/Ethidium Bromide (AO/EB), showing viable cells (green) with no signs of apoptosis.
E) Cur-AgNP-treated group stained with AO/EB. The treated cells exhibited apoptotic features (orange and green staining).
F) Quantification of live and dead cells in treated and control groups. The graph shows an increased proportion of dead cells in the treated group compared with the control. Arrows indicate apoptotic cells. Data are presented as mean±SD (magnification, ×200).

edly (to 54% relative expression) compared to untreated controls groups (p=0.001; Figure 4). These finding suggests Cur-AgNPs induced apoptosis and modulate gene expression by suppressing key inflammatory and extracellular matrix degrading enzyme, thereby contributing to their anti-angiogenic potential.

In-vivo assessment of ANT-angiogenic effects of Cur-AgNPs

Chick embryo chorioallantoic membrane: The chick embryo chorioallantoic membrane model was utilized to evaluate the inhibitory potential of Cur-AgNPs on angiogenesis. The treatment resulted in a clear dose-dependent suppression of neovascularization, as reflected by the progressive reduction in both the mean vessel length and vessel density in treated sample compared with untreated controls.

Specifically, administration of 50 *μg/ml* and 100 *μg/ml* Cur-AgNPs significantly reduced the mean vessel length to 33 and 27 *mm*, respectively, compared with 40 *mm* in the control group (p=0.04 and p=0.002).

A similar trend was observed for vessel number, which decreased to an average of 40 and 33 vessels at 50 *μg/ml* and 100 *μg/ml* Cur-AgNPs, respectively, compared with 54 vessels in controls (p=0.002 and p<0.001). In contrast, treatment with 25 *μg/ml* Cur-AgNPs (mean vessel number=49; p=0.19) did not pro-

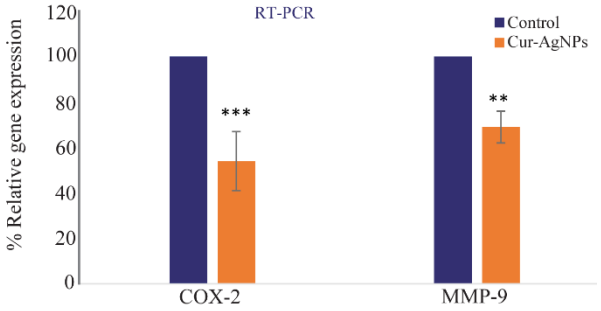

Figure 4. RT-PCR was performed to analyze the expression of *COX-2* and *MMP-9* genes in the control and the groups were treated by 13 *µg/ml* of Cur-AgNPs, (mean±SD), ***p≤0.001.

duce any significant alteration in vascularization, indicating a threshold concentration required for anti-angiogenic efficacy.

Evaluation of CAM vascularization and hemoglobin content

To further quantify vascular inhibition, hemoglobin content—an indirect indicator of vessel density—was determined using the Drabkin assay. A marked and statistically significant decrease in hemoglobin concentration was observed in CAMs treated with 50 *µg/ml* (mean=3.58) and 100 *µg/ml* (mean=2.50) Cur-AgNPs compared with untreated control (mean=3.90; p=0.006 and p=0.0001, respectively). The reduction in hemoglobin content was consistent with the observed decline in vessel number and length, suggesting effective vascular suppression (Figures 5 and 6). Collectively, these results provide compelling *in vivo* evidence of the potent anti-angiogenic activity of Cur-AgNPs. The findings imply that Cur-AgNPs effectively disrupt the formation and maturation of new blood vessels in a concentration-dependent manner, thereby supporting their potential.

Discussion

AgNPs were synthesized through an environmentally friendly approach using pure curcumin as both a reducing and capping agent [14]. The resulting nanoparticles exhibited a nearly spherical morphology with an average size of approximately 40 *nm*, as confirmed by TEM analysis, and displayed a negative zeta potential, indicating good colloidal stability. Fourier-transform infrared spectroscopy and energy-dispersive X-ray spectroscopy confirmed the successful conjugation of curcumin with AgNPs. Previous studies have reported the green synthesis of AgNPs using various plant extracts as reducing and stabilizing agents [15,16].

In the present study, pure curcumin was employed as a well-defined bioactive molecule for nanoparticle synthesis, in contrast to conventional approaches that rely on complex plant extracts. Similarly, Kabir *et al* [17] developed gold nanoparticles functionalized with silymarin, which acted as both a reducing and capping molecule, and the conjugation was verified using FTIR spectroscopy [17].

The inhibitory influence of Cur-AgNPs on angiogenesis was examined. The results revealed that Cur-AgNPs possess potent anti-angiogenic activity both *in vivo* and *in vitro* in a dose-dependent manner. Based on the findings from the CAM assay, Cur-AgNP treatment significantly reduced both the length and density of blood vessels on the chorioallantoic membrane. Furthermore, these nanoparticles markedly suppressed the proliferation of endothelial cells. To gain insight into the molecular mechanisms underlying this anti-angiogenic effect, the expression of *COX-2* and *MMP-9*—two principal genes involved in angiogenesis and metastasis—was analyzed in Cur-AgNP–treated endothelial cells and compared with untreated controls. The expression of both *MMP-9* and *COX-2* was found to be substantially downregulated following exposure to Cur-AgNPs. Proteolytic enzymes belonging to the MMP family, particularly MMP-2 and MMP-9, are known to participate in extracellular matrix degradation, facilitating tumor invasion and vascular development. Consequently, inhibition of these enzymes can effectively limit endothelial cell migration and the formation of new blood vessel [18,19].

Consistent with the present findings, several previous studies have reported the inhibitory effects of curcumin on *MMP-2*, *MMP-9*, and *COX-2* expression [20,21]. Similarly, Gurunathan *et al* [22] demonstrated that AgNPs suppress angiogenesis by inhibiting the activation of the PI3K/Akt signaling pathway and MMP-2 [22]. In

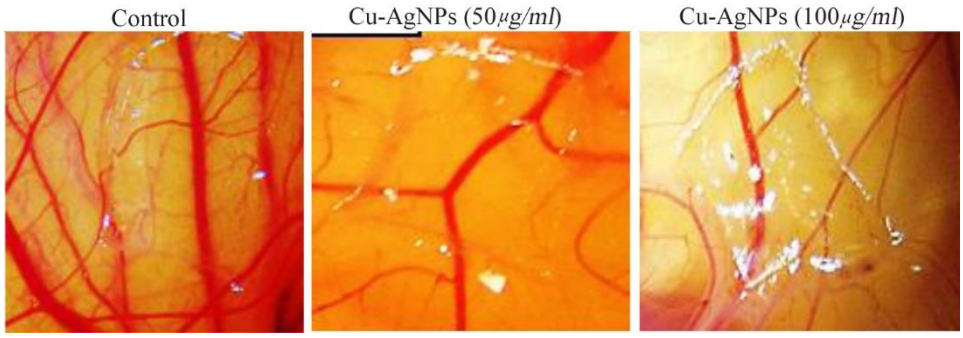

Figure 5. Average number and length of blood vessels in Chorioallantoic Membrane (CAM) samples were treated by different concentration of Cur-AgNPs compared to control.

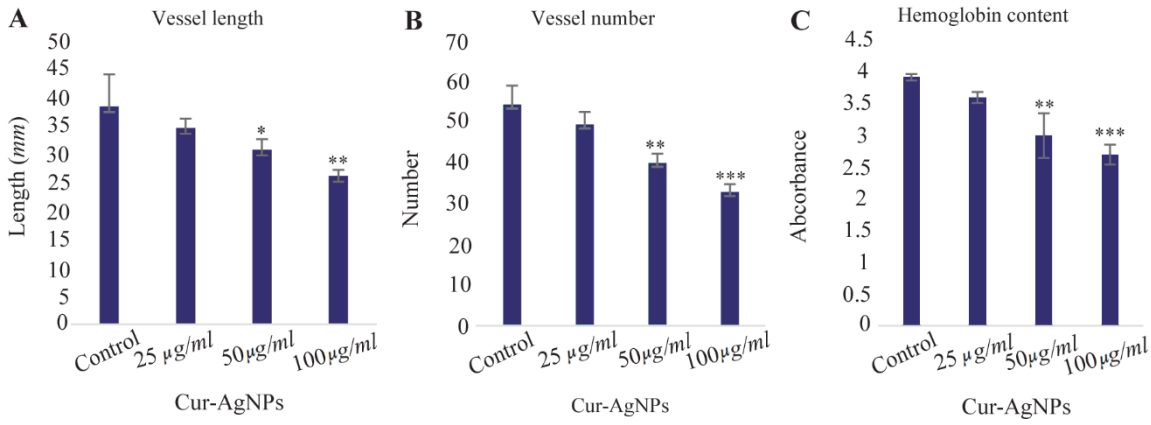

Figure 6. Effect of Cur-AgNPs on CAM angiogenesis.
A) Average length of CAM blood vessels in samples treated with different concentrations of Cur-AgNPs compared with the control. The results indicate a dose-dependent decrease in CAM blood vessel length. Treatment with 50 and 100 *µg/ml* Cur-AgNPs led to a significant reduction in vessel length compared with the control.
(B) Average number of CAM blood vessels in treated and control samples. A significant decrease in vessel number was observed at 50 and 100 *µg/ml* Cur-AgNPs compared with the control.
(C) Hemoglobin content measured using the Drabkin method. Samples treated with 100 *µg/ml* Cur-AgNPs showed a significant decrease in hemoglobin content relative to the control, indicating reduced angiogenesis.
Data are presented as mean±SD. *p≤0.05, p≤0.01, *p≤0.001.

another investigation, Satapathy and colleagues developed hybrid AgNPs functionalized with quinacrine (QAgNPs) and assessed their anti-tumor potential in several oral cancer cell lines, including H-357, Oral Squamous Cell Carcinoma (OSCC), and Oral Cancer Stem Cells (OSCC-CSCs), using both *in vitro* and *in vivo* models. Their results revealed that QAgNPs exhibited superior cytotoxicity toward OSCC-CSCs and produced a more pronounced reduction in angiogenesis compared to either quinacrine or AgNPs alone [23].

Furthermore, Ajaykumar *et al* [24] evaluated the anti-angiogenic potential of AgNPs synthesized using *Uvaria narum* extract (Un-AgNPs) through a CAM assay, reporting a marked inhibition of neovascularization. These observations are in strong agreement with the results obtained in the present study. Despite the promising outcomes, this work has certain limitations. The current experiments were restricted to *in vitro* and *in vivo* settings, which, although informative, do not fully replicate complex physiological conditions. Therefore, additional studies employing animal models and, ultimately, clinical trials are necessary to evaluate the long-term safety, systemic distribution, and potential toxicity of Cur-AgNPs. Future investigations should also explore their performance in cancer models to assess their feasibility as targeted nanocarriers for site-specific drug delivery. Comparative analyses with conventional chemotherapeutic and anti-angiogenic agents could further clarify the therapeutic advantages and translational potential of these nanoparticles. Addressing these aspects will strengthen and extend the significance of the current findings.

On the same note, the inhibitory effects of curcumin on *MMP-2, MMP-9,* and *COX-2* have been reported in previous studies [20,21]. In this regard, research by Gurunathan *et al* demonstrated that AgNPs exert inhibitory effects on angiogenesis, noting that AgNPs could inhibit the activation of PI3K/Akt and MMP. In another study prepared hybrid AgNPs (Agnos) by molecule quinacrine (QC) and evaluated the anti-tumor activity of QAgNPs using various cell lines, including H-357 oral cancer, oral squamous cell carcinoma (OSCC) and Oral Cancer Stem Cells in *in vivo* and *in vitro* model systems. According to their findings, QAgNPs have greater ability in killing OSCC-CSCs compared to QC and AgNPs alone. Furthermore, they reported that QAgNPs reduced angiogenesis more significantly compared to QC and AgNPs [23,25]. Ajaykumar *et al* [24] examianed the anti-angiogenic effects of AgNPs fabricated using *Uvaria narum* (Un-AgNps) extract.

For evaluating the anti-angiogenic effect of Un-AgNps the CMA was used. According to the results of this study, Un-AgNps show perfect anti-angiogenesis properties. These findings are consistent with the results of the present study [24].

Although this study provides valuable insights into the effects of AgNPs on HUVECs and CAMs, several limitations should be acknowledged. The current investigation was confined to *in vitro* and *in vivo* models, which, although informative, may not fully replicate the complexity of physiological conditions in living organisms. Therefore, future studies involving animal models and, ultimately, clinical trials are required to comprehensively assess the long-term safety, systemic distribution, and potential toxicity of AgNPs. Further investigations should also explore their behavior in tumor-bearing models to evaluate their potential as targeted nanocarriers for site-specific drug delivery.

Moreover, comparative studies with conventional chemotherapeutic and anti-angiogenic agents would offer a more holistic understanding of the therapeutic potential of AgNPs. Addressing these aspects will help to validate and extend the current findings.

Conclusion

In the present study, AgNPs were produced using pure curcumin as a non-ionic reducing agent. These nanoparticles were suitable in size for biological applications (39 *nm*) and also had good stability in aqueous environments (negative zeta potential). The results indicated that Cur-AgNPs induce apoptotic effects on HUVECs leading to inhibition of angiogenesis. Also *in vivo* CAM assay results confirm anti-angiogenesis properties of Cur-AgNPs. Overall, Cur-AgNPs show promise for future investigation in anti-angiogenesis and anti-cancer applications, although additional studies are required to fully understand therapeutic potential and safety.

Conflict of Interest

The authors declare no conflict of interest.

References

1. Kubota Y. Tumor angiogenesis and anti-angiogenic therapy. Keio J Med 2012;61(2):47-56.
2. Ghasemali S, Farajnia S, Barzegar A, Rahmati-Yamchi M, Baghban R, Rahbarnia L, et al. New Developments in Anti-Angiogenic Therapy of Cancer, Review and Update. Anticancer Agents Med Chem 2021;21(1):3-19.
3. Carmeliet P. Angiogenesis in life, disease and medicine. Nature 2005 Dec 15;438(7070):932-6.
4. Su J, Zhu HL, Yao Y, Duan Y. Antiangiogenic therapy: challenges and future directions. Ctmc 2021 Jan 1;21:87-9.
5. Bhandarkar SS, Arbiser JL. Curcumin as an inhibitor of angiogenesis. Adv Exp Med Biol 2007;595:185-95.
6. Bhatia M, Bhalerao M, Cruz-Martins N, Kumar D. Curcumin and cancer biology: Focusing regulatory effects in different signalling pathways. Phytother Res 2021 Sep;35 (9):4913-4929.
7. Gangwar RK, Tomar GB, Dhumale VA, Zinjarde S, Sharma RB, Datar S. Curcumin conjugated silica nanoparticles for improving bioavailability and its anticancer applications. J Agric Food Chem 2013 Oct 9;61(40): 9632-7.
8. Ghosh S, Dutta S, Sarkar A, Kundu M, Sil PC. Targeted delivery of curcumin in breast cancer cells via hyaluronic acid modified mesoporous silica nanoparticle to enhance anticancer efficiency. Colloids Surf B Biointerfaces 2021 Jan;197:111404.
9. Zhang L, Zhu W, Yang C, Guo H, Yu A, Ji J, et al. A novel folate-modified self-microemulsifying drug delivery system of curcumin for colon targeting. Int J Nanomedicine 2012;7:151-62.
10. Ullah H, Zulfiqar S, Khan MJ, Arshad Y, Abid R, Khan AA, et al. Evaluation of Photoactivated Curcumin Loaded Self Emulsifying Drug Delivery System In In Vitro Microbial Caries Model Against Enterococcus Faecalis. Journal of Pharmaceutical Negative Results 2023 Oct 1;14(4).
11. Xu L, Wang YY, Huang J, Chen CY, Wang ZX, Xie H. Silver nanoparticles: Synthesis, medical applications and biosafety. Theranostics 2020 Jul 11;10(20):8996-9031.
12. Lokina S, Stephen A, Kaviyarasan V, Arulvasu C, Narayanan V. Cytotoxicity and antimicrobial activities of green synthesized silver nanoparticles. Eur J Med Chem 2014 Apr 9;76:256-63.
13. Dawadi S, Katuwal S, Gupta A, Lamichhane U, Thapa R, Jaisi S, et al. Current research on silver nanoparticles: synthesis, characterization, and applications. Journal of Nanomaterials 2021;2021(1):6687290.
14. Ramezani T, Nabiuni M, Baharara J, Parivar K, Namvar F. Sensitization of Resistance Ovarian Cancer Cells to Cisplatin by Biogenic Synthesized Silver Nanoparticles through p53 Activation. Iran J Pharm Res 2019 Winter; 18(1):222-231.
15. Alharbi NS, Alsubhi NS, Felimban AI. Green synthesis of silver nanoparticles using medicinal plants: Characterization and application. Journal of Radiation Research and Applied Sciences 2022 Sep 1;15(3):109-24.
16. Huq MA, Ashrafudoulla M, Rahman MM, Balusamy SR, Akter S. Green Synthesis and Potential Antibacterial Applications of Bioactive Silver Nanoparticles: A Review. Polymers (Basel) 2022 Feb 15;14(4):742.
17. Kabir N, Ali H, Ateeq M, Bertino MF, Shah MR, Franzel L. Silymarin coated gold nanoparticles ameliorates CCl 4-induced hepatic injury and cirrhosis through down regulation of hepatic stellate cells and attenuation of Kupffer cells. RSC Advances 2014;4(18):9012-20.
18. Latronico T, Petraglia T, Sileo C, Bilancia D, Rossano R, Liuzzi GM. Inhibition of MMP-2 and MMP-9 by Dietary Antioxidants in THP-1 Macrophages and Sera from Patients with Breast Cancer. Molecules 2024 Apr 10;29 (8):1718.
19. Scoditti E, Calabriso N, Massaro M, Pellegrino M, Storelli C, Martines G, et al. Mediterranean diet polyphenols reduce inflammatory angiogenesis through MMP-9 and COX-2 inhibition in human vascular endothelial cells: a potentially protective mechanism in atherosclerotic vascular disease and cancer. Arch Biochem Biophys 2012 Nov 15;527(2):81-9.
20. Pricci M, Girardi B, Giorgio F, Losurdo G, Ierardi E, Di Leo A. Curcumin and Colorectal Cancer: From Basic to Clinical Evidences. Int J Mol Sci 2020 Mar 29;21(7): 2364.
21. Villegas C, Perez R, Sterner O, González-Chavarría I, Paz C. Curcuma as an adjuvant in colorectal cancer treatment. Life Sci 2021 Dec 1;286:120043.
22. Gurunathan S, Lee KJ, Kalishwaralal K, Sheikpranbabu S, Vaidyanathan R, Eom SH. Antiangiogenic properties of silver nanoparticles. Biomaterials 2009 Oct 1;30(31): 6341-50.
23. Satapathy SR, Siddharth S, Das D, Nayak A, Kundu CN. Enhancement of Cytotoxicity and Inhibition of Angio-

genesis in Oral Cancer Stem Cells by a Hybrid Nanoparticle of Bioactive Quinacrine and Silver: Implication of Base Excision Repair Cascade. Mol Pharm 2015 Nov 2;12(11):4011-25.

24. Ajaykumar AP, Mathew A, Chandni AP, Varma SR, Jayaraj KN, Sabira O, et al. Green Synthesis of Silver Nanoparticles Using the Leaf Extract of the Medicinal Plant, Uvaria narum and Its Antibacterial, Antiangiogenic, Anticancer and Catalytic Properties. Antibiotics (Basel) 2023 Mar 13;12(3):564.
25. Satapathy SR, et al. (2015) Enhancement of Cytotoxicity and Inhibition of Angiogenesis in Oral Cancer Stem Cells by a Hybrid Nanoparticle of Bioactive Quinacrine and Silver: Implication of Base Excision Repair Cascade', Molecular Pharmaceutics, 12(11),pp.4011-4025.